Precision Analysis of Terrestrial Reference Frame Parameters Based on EOP A-Priori Constraint Model

Jiao Liu[1,2], Junping Chen[1,2](✉), and Bin Wang[1]

[1] Shanghai Astronomical Observatory, Chinese Academy of Sciences,, Shanghai, China
junping@shao.ac.cn
[2] University of Chinese Academy of Sciences, Beijing, China

Abstract. Earth Orientation Parameters (EOPs) are quantitative parameters that reflect the Earth spatial motion and its rates along the rotation axes. Precession and nutation parameters can be precisely described by the theoretical model, while the complex variation of the pole motion and LOD (length of day) is difficult to be modelled and hard to be predicted with high precision. With the development of Global Navigation Satellite System (GNSS), the spatial and temporal resolution of EOP products have been greatly improved. In GNSS data analysis, a-priori EOPs are normally used as the prediction from the IERS, and the constraint applied on a-priori EOP parameters has much impact on the estimates of GNSS solutions. This paper studies this impacts and develops an a-priori EOP constraint model. GPS data of 142 evenly distributed IGS stations from the beginning of 2010 to the end of 2015 are used for data analysis. Firstly, the precision of the pole motion, LOD and station coordinates under two mostly-used constraint conditions are compared and analyzed, which proves the impact of a-priori EOP constraint on GNSS solutions. Secondly, an a-priori EOP constraint model (pole motion composed of four periodical terms, while LOD composed of two periodical terms) is then developed, where the periodical terms are determined using the Least Square Spectrum Analysis (LSSA) approach. Lastly, the new model is used as the constraint conditions in GNSS solutions. Compared with above two mostly-used constraints, the pole motion and LOD parameters under the new constraint model is closer to the IGS products with largest improvement of 75%, which demonstrates that the new EOP a-prior constraint model can effectively improves the precision of GNSS parameters.

Keywords: EOPs · TRF · Pole motion · LOD · LSSA · EOP a-prior constraint model

1 Introduction

Earth rotation parameters are quantitative parameters that reflect the motion of the Earth's Rotation axis in the Earth's body and the variation of Earth's rotation rate, together with precession and nutation constitute Earth Orientation Parameters (EOPs) that describe the long-term variation of Earth's rotation [1, 2]. The International Earth

J. Sun et al. (Eds.): CSNC 2020, LNEE 651, pp. 378–388, 2020.
https://doi.org/10.1007/978-981-15-3711-0_33

Rotation Service (IERS) regularly publish EOPs, including EOP products such as Bulletin A, Bulletin B/C04 and long-term C01, determined by several space geodetic techniques [3, 4]. Compared with EOPs provided by VLBI (Very Long Baseline Interferometry), SLR (Satellite Laser Ranging) and DORIS (Doppler Orbitography and Radio positioning Integrated by Satellite), those provided by the GNSS technology have higher spatial and temporal resolutions.

Accuracy of the EOPs is of great importance in scientific research and practical application. In deep space exploration and satellite precise orbit determination, high-precision EOPs are the prerequisites for the conversion of celestial coordinate system and earth coordinate system [5]. However, EOPs provided by IERS has a latency of several weeks, so that practical applications such as satellite orbit determination and GNSS data processing can only use its prediction as a-priori inputs.

In GNSS data processing, a-priori EOPs from the IERS are taken as inputs, and constrained to get the final results. Therefore, the precision of the prior values affect the precision of terrestrial reference frame including the EOPs. In this paper, we use the GNSS data processing software GAMIT/GLOBK, jointly developed by Massachusetts Institute of Technology (MIT) and Scripps Institution of Oceanography (SIO) [6–8], to analyze the effects of a-priori EOP constraints on the precision of GNSS solutions such as station coordinates, pole motions and length of day. The a-priori EOP constraint model is developed to improve the parameter estimation accuracy.

2 GNSS Based EOP Solution

The GAMIT/GLOBK GNSS software package is based on the Kalman filter algorithm. The function model of carrier phase observations is [9–11]:

$$L = M\left(t, X_{SP}, X_T, X_N, X_{erp}, X_{atm}\right) + \varepsilon \tag{1}$$

Where, M represents the function model of observations and the parameters to be estimated; t is one certain epoch; X_{SP} is the orbit elements and perturbation parameters at the initial epoch; X_T is the coordinate of the stations; X_N is the phase ambiguity; X_{erp} is the earth rotation parameters, including the pole motion parameters X_P, Y_P and D_R; X_{atm} is atmospheric delay; ε is the observation noise [12, 13].

The linearization of formula (1) is as follows:

$$L = C_0 + \frac{\partial M}{\partial X_{SP}} dX_{SP} + \frac{\partial M}{\partial X_T} dX_T + \frac{\partial M}{\partial X_N} dX_N + \frac{\partial M}{\partial X_{erp}} dX_{erp} + \frac{\partial M}{\partial X_{atm}} dX_{atm} + \varepsilon \tag{2}$$

In formula (2), C_0 is initial value, and partial derivatives of the earth rotation parameters is $\frac{\partial M}{\partial X_{erp}} = \frac{\partial M}{\partial \rho} \frac{\partial \rho}{\partial R_I} \frac{\partial R_I}{\partial X_{erp}} = \frac{(r - R_I)}{\rho} \frac{\partial R_I}{\partial X_{erp}}$. r and R_I are respectively satellite and station position in inertial coordinate system; ρ is distance between satellite and station; $\frac{\partial R_I}{\partial X_{erp}}$ including $\frac{\partial R_I}{\partial X_P}$, $\frac{\partial R_I}{\partial Y_P}$ and $\frac{\partial R_I}{\partial D_R}$. X_P and Y_P are respectively the x and y component of pole motion.

Components of the station coordinates in x and y direction of the pole motion are as follows:

$$\frac{\partial R_I}{\partial X_P} = PNS\frac{\partial W}{\partial X_P}R_T(t) = PNS\begin{bmatrix} -z \\ 0 \\ x \end{bmatrix} \tag{3}$$

$$\frac{\partial R_I}{\partial Y_P} = PNS\frac{\partial W}{\partial Y_P}R_T(t) = PNS\begin{bmatrix} -X_P y \\ X_P x + z \\ -y \end{bmatrix} \tag{4}$$

In Eqs. (3) and (4), P and N are precession and nutation matrices; S is the earth rotation matrix; W is the polar motion matrix; $R_T = (x, y, z)$ is the station position vector in the earth fixed coordinate system.

The first-order variation rate for UT1-TAI, i.e. LOD, is expressed as D_R, and

$$\frac{\partial R_I}{\partial D_R} = \frac{\partial R_I}{\partial \theta_g}\frac{\partial \theta_g}{\partial D_R} \tag{5}$$

$$\frac{\partial R_I}{\partial \theta_g} = PN\frac{\partial S}{\partial \theta_g}W^T = PNSW\begin{bmatrix} -y - Y_P z \\ x - X_P z \\ Y_P x + X_P y \end{bmatrix} \tag{6}$$

$$\frac{\partial \theta_g}{\partial D_R} = 2\pi(1+k)\frac{\partial UT1}{\partial D_R} = 2\pi(1+k)(t - t_0) \tag{7}$$

$$\theta_g = GAST = 2\pi\begin{bmatrix} GMST(UT0) + \\ (1+k)UT1 \end{bmatrix} + \Delta\varphi cos\phi \tag{8}$$

Where $\theta_g = GAST$ is Greenwich apparent sidereal time; $GMST$ is Greenwich mean sidereal time; $\Delta\varphi$ is the nutation in longitude; ϕ is obliquity. The station coordinates and satellite orbit are obtained from IGS [14, 15].

3 EOP Precision Under Different Constraints

GPS data of 142 evenly distributed IGS stations were used, and the distribution is shown in Fig. 1. Station coordinates and EOPs are estimated using observations of six years from January 3, 2010 to December 20, 2015 (GPS week is 1565 to 1876). The seismic information used in data processing is consistent with ITRF2014, the antenna and receiver information are consistent with the stations log file, and the prior coordinate values are given by ITRF2014. In practical applications, the final solution of the IERS EOPs has a long latency period, and the rapid product published by IERS is used as the a-priori value.

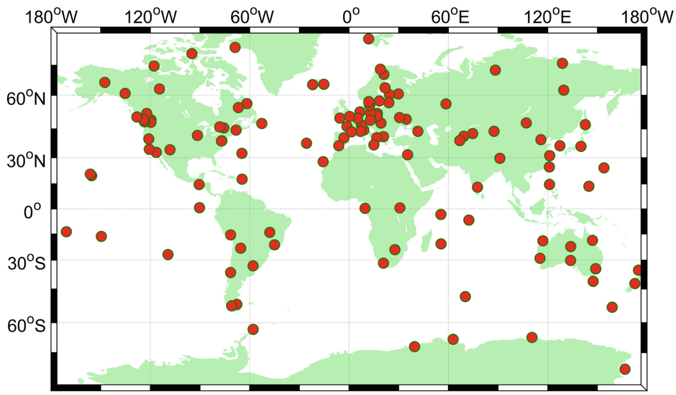

Fig. 1. Distribution of selected stations

Based on the above data, the TRFs are constructed under two different constraints of coordinates and pole motion as well as LOD. The two selected constraints are of great difference to reveal evident difference of coordinates and EOPs under different constraints and are shown in Table 1. For the sake of ensuring the consistency of the comparison results, the IG2 (IGS second reprocessing campaign) SINEX product was used when before GPS week 1831, while the IGS SINEX product was used when after GPS week 1831 as the reference for comparison. Analysis results of the paper are referred as SHA.

Table 1. Two different constraints

Constraint	Coordinate (N, E, U) m	Pole motion (Px, Py) mas	Pole motion rate (Pxr, Pyr) mas/yr	LOD ms
Constraint 1	1 1 1	5 5	1 1	1
Constraint 2	.01 .01 .01	1 1	.1 .1	.1

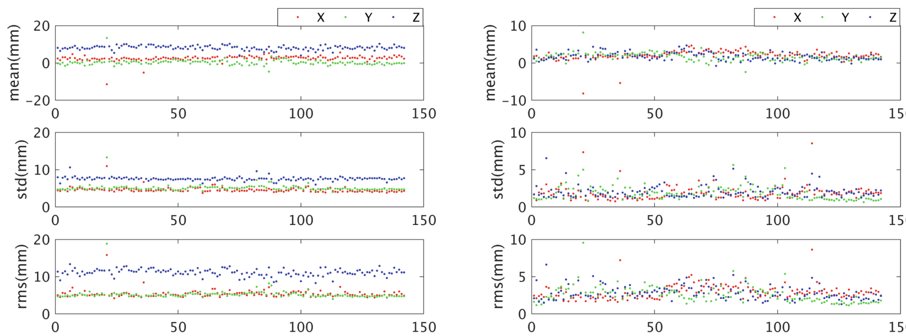

Fig. 2. Statistics of station coordinates accuracy, x axis represents the station index (left: constraint 1, right: constraint 2)

Under constraints 1 and 2, the mean, standard deviation and root mean square of coordinate differences between IGS and SHA for each station are shown in Fig. 2. Results show that under constraint 1, the error in X and Y component is about 5 mm, and the error in Z component is about 10–12 mm. Under constraint 2, the error of most stations in three components is within 2–5 mm. The mean value of both constraints is greater than zero, which is caused by the difference of station distribution and network shape for IGS and SHA solution. In general, the precision of station coordinates is higher under constraint 2, which reflects the rationality of station coordinates constraint.

Time series of pole motion difference and LOD difference between IGS and SHA under constraints 1 and 2 are respectively shown in Figs. 3 and 4, and corresponding statistics are shown in Table 2. Results show that, compared with constraint 1, the amplitude of harmonics and system bias of pole motion in the Y direction under constraint 2 are significantly reduced, and also for the amplitude of periodic term and slope of LOD difference.

All above show that the results under constraint 2 are closer to IGS products. The residual linear and nonlinear signals in Fig. 4 reveal the defects of the empirical constraints. Therefore, how to obtain relatively reasonable constraints is critical in the establishment of the TRF.

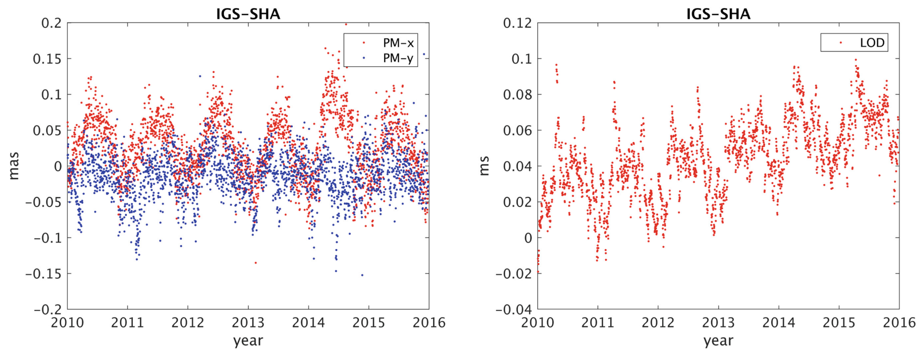

Fig. 3. Differences of pole motion and LOD Parameters under constraint 1

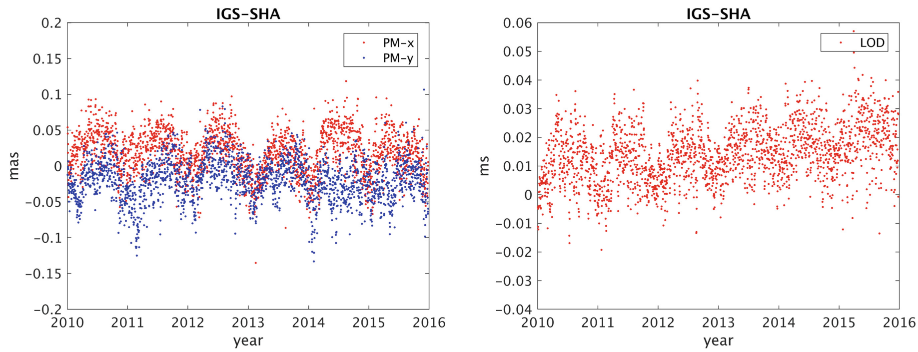

Fig. 4. Differences of pole motion and LOD Parameters under constraint 2

Table 2. Error statistics of pole motion and LOD parameters

	PM-x (mas)		PM-y (mas)		LOD (μs)	
	RMS	STD	RMS	STD	RMS	STD
Constraint 1	0.051	0.043	0.035	0.032	49.3	21.4
Constraint 2	0.035	0.030	0.035	0.029	17.2	9.9

4 The A-Priori EOP Constraint Model

As shown in Fig. 5, time series of the difference between the rapid EOP published by IERS and IGS EOP is obtained taking IGS EOP products as the reference. There are significant periodic characteristics in the pole motion differences, and the least square spectrum analysis (LSSA) is used to obtain the spectrum diagram, as shown in Fig. 6. In Fig. 6, the pole motion difference in the X direction and Y direction respectively contains two harmonics with almost the same amplitude. Fitting residuals after removing these two harmonics are shown in Fig. 7. And fitting residuals of LOD after removing the two harmonics with the largest two amplitude are shown in Fig. 8, in which the standard deviation of the LOD fitting residuals is 0.064 ms.

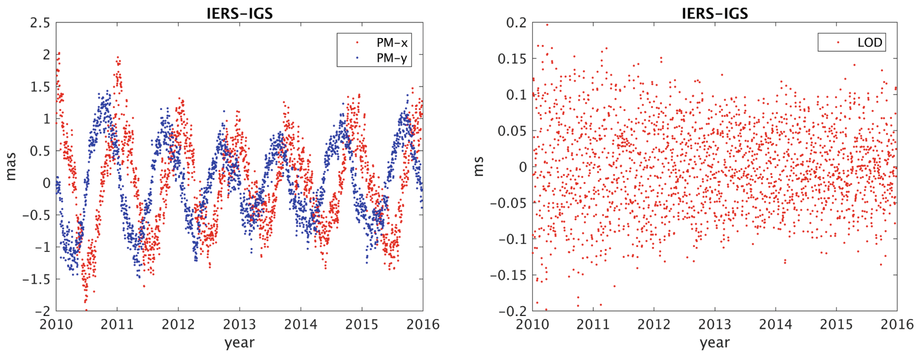

Fig. 5. Time series of the difference between IERS EOP rapid products and IGS EOP products

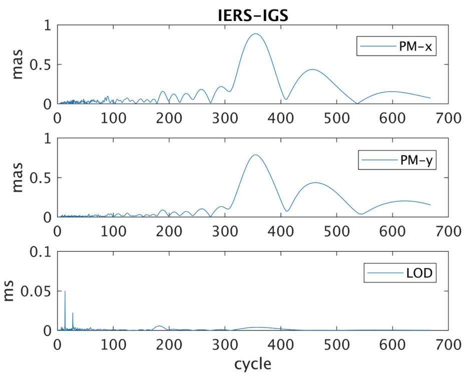

Fig. 6. Spectrums of the difference between IERS EOP rapid products and IGS EOP products

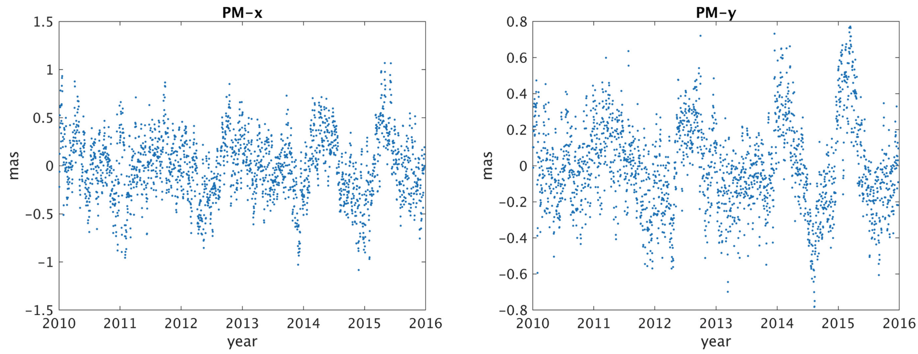

Fig. 7. Time series of pole motion parameters fitting residuals

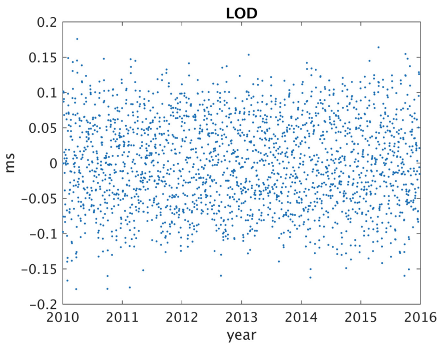

Fig. 8. Time series of LOD fitting residuals

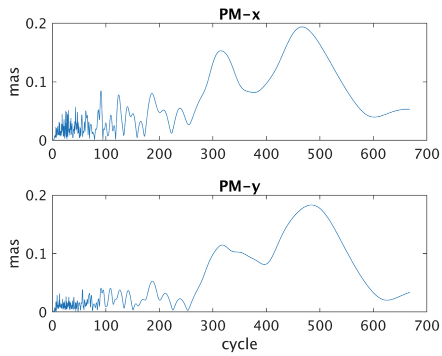

Fig. 9. Spectrums of pole motion parameters fitting residuals

However, the residuals in Fig. 7 still contains small harmonics. And the LSSA of the residuals in Fig. 7 is further performed, and the spectrum is shown in Fig. 9. Two harmonics with largest amplitude in Fig. 9 and two largest harmonics in Fig. 6 are selected to fit the time series of the differences between EOP products in Fig. 5. The fitting results and the residuals are shown in Figs. 10 and 11, respectively. Compared with Fig. 7, the periodic characteristic in the fitting residuals has disappeared, and the standard deviations of the fitting residuals are 0.288 mas and 0.199 mas, respectively for each components of pole motion.

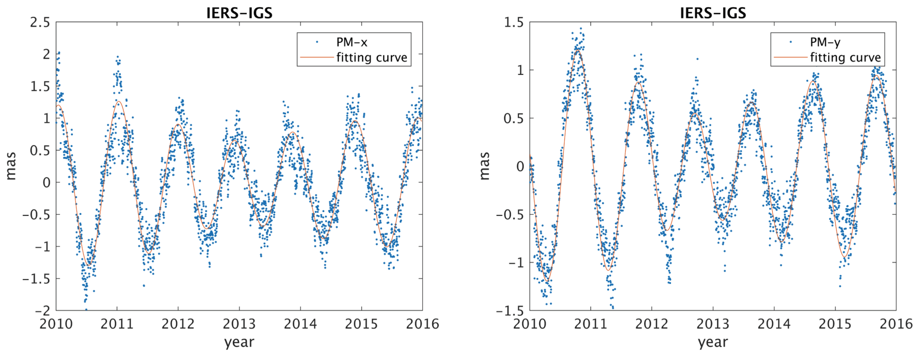

Fig. 10. Fitting results of the difference between IERS EOP rapid products and IGS EOP products

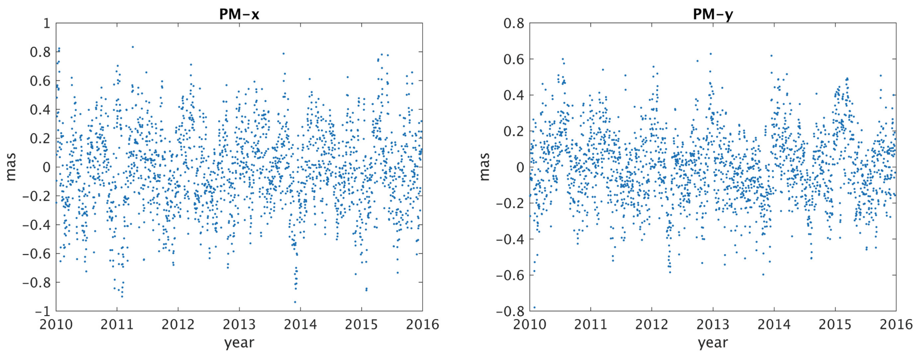

Fig. 11. Time series of pole motion parameters fitting residuals

With the harmonics obtained above and the standard deviation of the fitting residuals, the pole motion a-priori constraint model can be defined as:

$$\sigma_p = \left| \sum\nolimits_{i=1}^{4} A_i cos\left(\frac{2\pi}{T_i} + P_i\right) \right| + \sigma_r \tag{10}$$

Where A_i is the amplitude, T_i is the period in days, P_i is the phase in radian, and σ_r is the standard deviation of the fitting residuals. For the four harmonics of the polar motion in X and Y directions, the periods, amplitudes, phases and also the standard deviations of the fitting residual are shown in Table 3. The phases in Table 3 are based on modified Julian day.

Table 3. The periods, amplitudes, phases and fitting residual standard deviations of the pole motion

	PM-x			PM-y		
	Period (day)	Amplitude (mas)	Phase (rad)	Period (day)	Amplitude (mas)	Phase (rad)
Period 1	355.1	0.8885	−3.0520	354.8	0.7884	−2.3519
Period 2	456.5	0.4362	1.3713	461.9	0.4360	−0.5907
Period 3	315.2	0.1513	−1.7556	317.9	0.1147	2.9877
Period 4	466.4	0.1938	2.2057	484.1	0.1833	0.1287
Fitting residual	0.288 mas			0.199 mas		

The a-priori constraint model of LOD is defined as:

$$\sigma_l = \left| \sum\nolimits_{i=1}^{2} A_i cos\left(\frac{2\pi}{T_i} + P_i\right) \right| + \sigma_r \tag{11}$$

Meanings of parameters in Eq. (11) are consistent with those in Eq. (10). The periods, amplitudes, phases and standard deviations of fitting residuals for two harmonics of LOD are shown in Table 4.

Table 4. The periods, amplitudes, phases and fitting residual standard deviations of the LOD

	LOD		
	Period (day)	Amplitude (mas)	Phase (rad)
Period 1	13.7	0.0501	−1.1694
Period 2	27.5	0.0226	−2.2127
Fitting residual	0.064 ms		

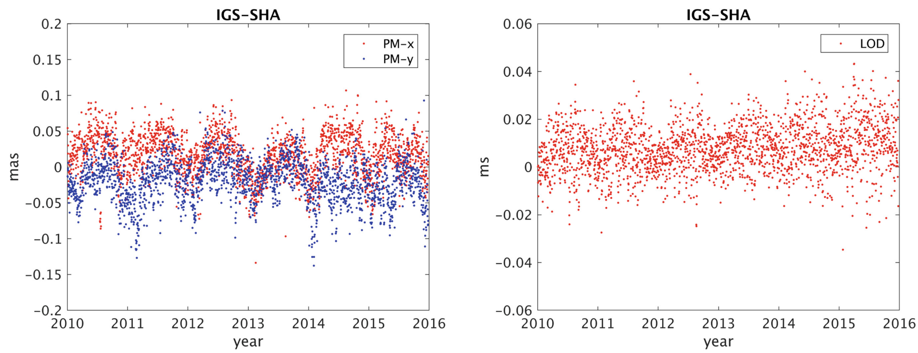

Fig. 12. Differences of pole motion and LOD Parameters under EOP a-priori constraint model

According to the analysis in Sect. 3, when the coordinate constraint is 1 cm, the coordinate accuracy is relatively high, and 1 cm coordinate constraint is used in this section. For the earth rotation parameters, above defined EOP a-priori constraint model is used to establish the global earth reference frame. The differences between the earth rotation parameter SHA and IGS products are shown in Fig. 12. In Fig. 12, the standard deviations of the pole motion in X and Y directions and also the LOD are 0.029 mas, 0.028 mas and 9.9 μs, and the root mean square error are 0.034 mas, 0.035 mas and 12.4 μs, respectively. Compared with constraint 2, the dispersion of the pole motion estimation has been decreased, the periodic characteristics of LOD is suppressed significantly, and the trend has also disappeared. Compared with constraint 1 and 2, the improvement percentage expressed by standard deviation and root mean square error of the pole motion and LOD parameters can be found in Table 5. Based on the above analysis, it can be concluded that estimation of the pole motion and LOD parameters under EOP a-priori constraint model are more consistent with the EOP products of IGS, which can greatly improve the parameter accuracy of GNSS daily solution.

Table 5. Percentage increase in pole motion and LOD parameters relative to constraint 1 and constraint 2

		PM-x	PM-y	LOD
RMS	Constraint 1	34.1%	0	74.85%
	Constraint 2	5.6%	0	27.9%
STD	Constraint 1	34.3%	13.5%	53.74
	Constraint 2	5.9%	2.4%	0

5 Conclusions

The EOPs are important parameters of TRF. In this paper, GAMIT/GLOBK is used to establish the TRF using GPS observations, and the EOP a-prior constraint model is presented to obtain relatively reasonable constraints. The application results of this model confirmed the availability of the EOP a-prior constraint model. The conclusions are as follows:

(1) When different constraints are applied on the station coordinates and the EOPs, estimation precision of TRF parameters are greatly different;
(2) Inappropriate constraint model would generate alias signals in the TRF parameter estimation;
(3) The EOP a-priori constraint model based on the LSSA method is more applicable;
(4) pole motion and LOD parameters under the new constraint model is more consistent with the IGS EOP products with largest improvement of 75%.

Acknowledgements. This research is supported by the National Natural Science Foundation of China (No. 11673050); the Key Program of Special Development funds of Zhangjiang National Innovation Demonstration Zone (Grant No. ZJ2018-ZD-009); National Key R&D Program of China (No. 2018YFB0504300); and the Key R&D Program of Guangdong province (No. 2018B030325001).

References

1. Wang, X., Yuan, Y., Tan, B., et al.: Estimation of the ERPS based on GPS data and the analysis of the impact factor. J. Geodesy Geodyn. **36**(10), 902–906 (2016)
2. Gambis, D.: Monitoring earth orientation using space-geodetic techniques: state-of-the-art and prospective. J. Geodesy **78**(4), 295–303 (2004)
3. Gambis, D., Johnson, T., Gross, R., et al.: General combination of EOP series. IERS Tech. Note **30**, 39–50 (2003)
4. Dick, W.R., Thaller, D.: IERS annual report 2012 (2014)
5. He, Z., Yang, X., Li, Z., et al.: Estimation of earth rotation parameters based on GPS observations. J. Time Freq. **33**(1), 69–96 (2010)
6. Department of Earth, Atmospheric, and Planetary Sciences, Massachusetts Institute of Technology: GAMIT reference manual, release 10.6[EB/OL], 21 June 2014. http://www-gpsg.mit.edu/~simon/gtgk/GAMIT_Ref.pdf
7. Department of Earth, Atmospheric, and Planetary Sciences, Massachusetts Institute of Technology: GLOBK reference manual, release 10.6[EB/OL], 21 June 2014. http://www-gpsg.mit.edu/~simon/gtgk/GLOBK_Ref.pdf
8. Massachusetts Institute of Technology: Documentation for the GAMIT GPS analysis software [EB/OL], 25 December 2012. http://www-gpsg.mit.edu/~simon/gtgk/GAMIT.pdf
9. Xu, G., Xu, Y.: GPS: Theory, Algorithms and Applications, 3rd edn. Springer, Berlin (2016)
10. Li, J.: Artificial Satellite Precision Track Determination. People's Liberation Army Press, Beijing (1997)
11. Liu, G.: Some key issues relating to high precision GPS positioning and crustal deformation analysis. Graduate University of Chinese Academy of Sciences (Institute of Measurement and Geophysics, Chinese Academy of Sciences, Wuhan (2004)
12. Kouba, J.: Testing of the IERS2000 sub-daily earth rotation parameter model. Stud. Geophys. Geod. **47**(4), 725–739 (2003)
13. Meindl, M., Dach, R., Thaller, D., et al.: The impact of the processing batch length in GNSS data analysis on the estimates of earth rotation parameters with daily and subdaily time resolution. EGU Gen. Assem. **14**, 8026 (2012)
14. Chen, J.: Towards the new century GPS. Aerosp. China **10**, 26–31 (2000)
15. Zhou, Z., Yi, J.: GPS Satellite Measurement Principle and Application. Surveying and Mapping Press, Beijing (1992)